Innovative Prepositioning and Dispatching Schemes of Electric Vehicles for Smart Distribution Network Resiliency and Restoration

Alghamdi, Abdullah; Jayaweera, Dilan

DOI:
10.1109/APPEEC53445.2022.10072198

License:
Other (please specify with Rights Statement)

Document Version
Peer reviewed version

Citation for published version (Harvard):
Alghamdi, A & Jayaweera, D 2023, Innovative Prepositioning and Dispatching Schemes of Electric Vehicles for Smart Distribution Network Resiliency and Restoration. in *2022 IEEE PES 14th Asia-Pacific Power and Energy Engineering Conference (APPEEC).*, 22881325, Asia-Pacific Power and Energy Engineering Conference, IEEE, pp. 1-6, 2022 IEEE PES 14th Asia-Pacific Power and Energy Engineering Conference (APPEEC), Melbourne, Victoria, Australia, 20/11/22. https://doi.org/10.1109/APPEEC53445.2022.10072198

Innovative Prepositioning and Dispatching Schemes of Electric Vehicles for Smart Distribution Network Resiliency and Restoration

Abdullah Ali M. Alghamdi, *Student Member, IEEE*
Dept. of Electronic, Electrical and System Engineering
University of Birmingham, Birmingham, United Kingdom
Taibah University, Yanbu, Medina, Saudi Arabia
axa1455@student.bham.ac.uk

Dilan Jayaweera, *Senior Member, IEEE*
Dept. of Electronic, Electrical and System Engineering
University of Birmingham
Birmingham, United Kingdom
d.jayaweera@bham.ac.uk

***Abstract*—Mobile power sources (MPS), such as electric vehicles (EVs), potentially improve distribution network (DN) restoration under extreme event conditions. However, employing EVs as a major power source is under researched, as is the prepositioning, routing, and dispatch of large numbers of EVs. This study proposes a three-stage optimization approach to achieve proactive prepositioning, dynamic routing, and dynamic power scheduling for effective assessment of resilience and needy restoration. First, EVs are prepositioned in the DN to enable swift pre-restoration and improve the survival of loads. Second, following an extreme event, EVs are dynamically routed in the DN and transportation system (TS) to improve system recovery. This stage also proposes a novel EV travelling model, bridging consumption rate and distance to study the efficacy of EV's state of charge (SOC) and the participation decision of the EV's user. Third, dynamic power scheduling of EVs is addressed, based on decisions made in the previous two stages. A mixed-integer programming model that addresses matters such as various timeframes of EV dispatch and DS operation, and the connection of road and power networks, is tested via case studies of a three-phase AC IEEE 123-node test system to demonstrate the effectiveness of the proposal.**

***Index Terms*—Dispatching, Distribution Networks (DNs), Electric Vehicles (EVs), Prepositioning, and Restoration.**

I. Introduction

In recent years, more frequent extreme events, such as hurricanes, have resulted in large-scale and long-duration power disruptions [1]–[3]. Conventional restoration practice alone may not be able to restore power to the loads affected in a timely manner, according to security standards in [4]. Specifically, distribution network (DN) disruptions account for nearly 70% of electric service outages [5]. Mobile power sources (MPSs), such as electric vehicles (EVs), can provide spatial flexibility to improve DN resilience. However, EV dispatch, which is simply a vehicle routing and scheduling problem, combined with DN restoration, is not well-investigated. The use of EVs to power islanded feeders during large-area and long-duration outages is justified by industry-relevant practices [6]–[13], and is encouraged by related organizations and authorities, as in [14]. This is due to their considerable potential to improve DN resilience during abnormal operation conditions. While the extant literature in the field considered the effects of EVs on electric service reliability during ordinary outages, namely '$(N-1)$ criterion', there are currently only limited studies regarding EV routing and scheduling for promoting a robust response to extreme events. For example, the authors in [15]–[17] applied proactive EV dispatching procedure, but did not use EVs as primary sources to improve the survival of the electrical supply to loads, and to concurrently enhance the system service recovery. Meanwhile, related works such as [18]–[20] integrated different EV operating modes, such as vehicle-to-grid (V2G), while considering different types of user behaviour for restoration. However, these strategies where not examined for a major or total blackout, namely resiliency assessment. Overall, to the best of the present researchers' knowledge, no existing study evaluated a large number of EVs individually as a primary source of DN resilience and restoration, and no existing studies integrated different types of charging stations (CSs) and EV characteristics alongside human behaviour in the restoration process. This paper proposes an innovative three-stage mixed-integer programming framework to address some of the limitations of the models currently available in smart power distribution network restoration using EVs. The main contributions of the paper are as follows:

- A proactive prepositioning stage is proposed, in which each EV is prepositioned independently, according to the real data exchanged between the distribution network operators (DNOs) and the charging stations operators (CSOs). This framework implicitly considers each EV's user participation decisions, in order to replicate the EV's user behaviour during the restoration process;
- The state of charge (SOC), location, and optimal paths of EVs are determined and integrated into the routing stage, in order to distribute EVs optimally, maintaining the critical route that maximizes the total sum of restored load. The decisions made in the preceding steps are incorporated into the scheduling stage, where the objective is

to reduce the overall restoration cost. The negative effects of blackouts, and the restoration effect of the black-start scheme are assessed intuitively using economic means.

II. Problem Formulation

Disasters can cause the partial or complete loss of power supply from the main grid to DNs. These incidents can cause direct and indirect impacts on power system infrastructure, such as transmission system and substations outages and severe damage to the components of a DN, such as the feeders or laterals. Since these major impacts affect the conventional top-down restoration strategies, the use of reliability metrics is not suitable for enhancing DN performance after a major blackout. Instead, bottom-up, resiliency-oriented restoration strategies are an effective way of assessing how stationary and/or MPS can be utilized to avoid prolonged power outages shortly after extreme events, in which they are an effective response to addressing power sources to enhance power supply survivability and system service recovery [21]. The conceptual resilience trapezoid curve employed in [22] is presented in Fig. 1 to clarify the the significant of the proposed restoration strategy in terms of enhancing the smart DN resilience over time. As the figure shows, a distribution network performance (R) changes as it passes through the different states resulting from an associated extreme disaster. These states are resilience state $t_0 \sim t_e$, extreme event progress $t_e \sim t_{pe}$, post event state (namely, degraded state) $t_{pe} \sim t_r$, restorative state $t_r \sim t_{pr}$, post-restorative state $t_{pr} \sim t_{ir}$, and the DN's infrastructure recovery phase $t_{ir} \sim t_{pir}$. Since the post-event state consists of three consecutive stages, (1) the post-event state $t_{pe} \sim t_p$, in which rapid pre-restoration can be carried out immediately following the disaster, such as dispatching EVs and connecting energy storage systems (EESs) and distributed generators (DGs); (2) the pre-restoration state $t_p \sim t_{pp}$; and (3) the post-restoration state , this study proposes a three-stage optimization framework to implement proactive EV prepositioning, dynamic routing, and the dynamic power scheduling of each EV as an MPS, considering travelling time, and EV users' participation decisions. In this study, each EV's connection status can be either 'connected' (namely, the EV is plugged into a charging slot and ready for discharging at t_0), or 'disconnected' (namely, the EV is not plugged into a charging slot at t_0). The connected EVs are maximized in the prepositioning stage, while EVs whose SOC is insufficient for participation, or whose owners decide not to participate, are excluded from the restoration process demonstrated. Additionally, the users of disconnected EVs, namely EVs in travelling status, are encouraged to participate in the restoration operations. If the user of the disconnected EV chooses to participate, and their EV's estimated SOC level is sufficient when it arrives at the charging slot, the user will share the coordinates of the closest accessible charging slot determined in the first stage, and the critical route obtained in the second stage. Therefore, the connection time and location of each EV can be used for the third stage, namely the dynamic power scheduling. The problem formulation presented in this section is supported by the practices of industries that involve the use of EVs to power an islanded feeder during large-area and long-duration outages [6]-[13], as well as those of the relevant authorities [14], and academia [15]-[18], [24], [25].

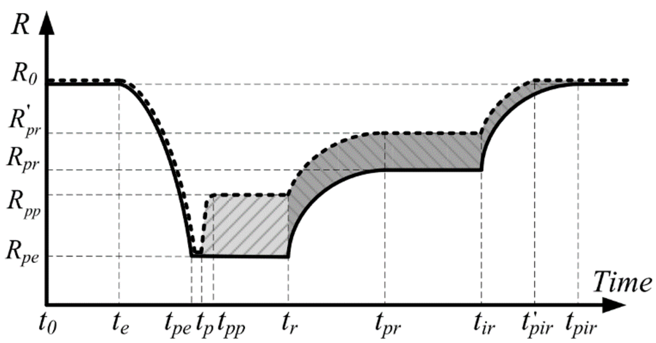

Fig. 1. The conceptual resilience trapezoid curve during an event [22].

A. Proactive Prepositioning of EVs

The first stage (resilience state $t_0 \sim t_e$), namely prior to the event, involves collecting data for proactive prepositioning, in which EVs are prepositioned depending on the data obtained by the DNOs, for example the component's status, such as the feeders and laterals, and that of the CSOs, for instance the CSs and EVs available. At this stage, the communication infrastructure is expected to be operationally normal, with data recorded automatically by the CSO, and transmitted continuously to the DNO, for proactive prepositioning. Table I shows the two types of data that can be used for prepositioning, namely station records and charging records [11]. The charging record is generated by measuring each user's charging session, whereas the station record is collected directly from the charging station. This data is utilized in this study to obtain (1) the magnitude: the amount of power available in each EV's battery to be discharged; (2) the frequency: the EV's connection frequency, which can be used to forecast the consumer's participation decision; and (3) the duration: the EV's connection duration that is sufficient to discharge the power of each EV while in V2G mode. The pre-positioning of EVs can enhance load survivability and improve the resilience performance index (RPI) from R_{pe} to R_{pp} , as shown by the dotted line in Fig. 1. In contrast, in the absence of a proactive preposition approach, the post-event resilience level remains at R_{pe} , until t_r , which is shown in Fig. 1 by the solid line. EVs is prepositioned in the DN prior to the extreme event, in order to improve its survivability. To evaluate the prepositioning strategy, a three-stage robust optimization model is proposed. At t_e , the objective is to maximize the amount of load restored immediately following the assessment of system damages and outages. In this stage, the objective function is formulated to maximize the sum weighted of survived loads as follows:

$$\max \sum_{\forall t} \sum_{\forall i} \sum_{\forall \phi} P^{L}_{i,\phi,t}, \forall t \in T, \forall i \in N, \forall \phi \in \Phi \tag{1}$$

TABLE I
DATA RECORDED BY CHARGING OUTLETS

Charging station records	**Electric vehicle records**
Location	Charging and Discharging rates
Typical charging speed	EV's battery status (SOC)
Capacity (in terms of EV)	EV's battery status (DoD)
Connection status	
Power ratings	Participation rate (user's decision)
Typical charge time	
Available charging slots	Energy consumption rate

where $P^L_{i,\phi,t}$ is the active power demand at node i and phase ϕ at time t. Since the EVs have different locations and SOC levels, the connected EVs rapidly discharge the power to the grid (namely, V2G mode) to increase the sum weight of the survived load. The constraints involved in this stage are:

$$x^{Pre}_{i,g,t} = 1, \forall g \in G^{EV}, \forall i \in N^{CS}, t = 1 \tag{2}$$

$$\sum_{\forall g \in G^{EV}} x^{Pre}_{i,g,t} = CSC^{CS}_{i,t}, \forall i \in N^{CS}, t = 1 \tag{3}$$

$$CSC^{min}_{i,t} \leq CSC^{CS}_{i,t} \leq CSC^{max}_{i,t}, \forall i \in N^{CS}, t = 1 \tag{4}$$

where $x^{Pre}_{i,g,t}$ is a binary variable that indicates the EV's g connection status to node i prior to the event (at $t = 1$). Constraint (2) enforces the fact that each connected EV is prepositioned to exactly one of its candidate CS at $t = 1$. Constraints (3) and (4) limit the number of connected EVs to each CS during the prepositioning stage. The CS capacity limit ($CSC^{CS}_{i,t}$) is a variable in which the CS capacity changes over time, according to the number of EVs connected at each t. The radiality constraints in [26] are involved in this stage, to determine the set of damaged lines.

B. Dynamic Routing of EVs

In the second stage, the dynamic routing is conducted to route EVs to the designated CS in stage-I, via the critical path, in order to minimize the travelling time and energy consumption rate during travel. The TS is considered to be operationally normal at this stage, and the routes that EVs can use, namely according to the road map, are aligned with the DN's lines. In the dynamic network reconfiguration, the power dispatch of the DN is co-optimized in this stage to coordinate with the restoration strategy and the efforts of infrastructure recovery, in order to enhance the DN's RPI from t_{ir} to t_{pir}. The objective function of this stage is to minimize the route path (x^{EV}_{route}) required for travelling by each EV from its allocated coordinates in stage-I to the closest available charging station:

$$x^{EV}_{route} = \arg\min \left\{ \sum_{\forall i \in N^{CS}} \sum_{\forall g \in G^{EV}_{ev}} t^{travil}_{(i,j))} \right\} \tag{5}$$

where an EV's g travelling status ($t^{travil}_{(i,j))}$) equals 1 if it is not connected to a charging station, otherwise it is 0. The values obtained for x^{EV}_{route} are used in stage-III by setting the connection time and the associated charging station for each EV. The constraints involved in this stage are:

$$\sum_{\forall g \in G^{EV}_{ev}} x^{Post}_{(i,j)} = CSC^{CS}_{i,t}, \forall i \in N^{CS}, \forall t \tag{6}$$

$$CSC^{min}_{i,t} \leq CSC^{CS}_{i,t} \leq CSC^{max}_{i,t}, \forall i \in N^{CS}, \forall t \tag{7}$$

$$\sum_{\forall i \in N^{CS}} x^{Post}_{i,g,t} \leq 1, \forall g \in G^{EV}_{ev}, \forall t \tag{8}$$

Constraints (6)-(8) limit the number of EVs connected to each CS after the prepositioning stage ($t > 1$). Meanwhile, the binary variable $x^{Post}_{i,g,t}$ indicates the EV's g connection status shortly after the disaster. It is important to note that being connected to the DN and moving on the TS are mutually exclusive and collectively exhaustive states of an EV in each time period. The following equations reflect this relationship, where $t^{travil}_{(i,j),g}$ is the travelling time of an EV

$$t^{travel}_{(i,j),g} = 1 - \sum_{\forall i \in N^{CS}} x^{Post}_{i,g,t}, \forall g \in G^{EV}_{ev}, \forall t \tag{9}$$

$$x^{Post}_{i,g,t+\tau} + x^{Post}_{i,g,t} \leq 1, \forall i \in N^{CS}, \forall g \in G^{EV}_{ev}, t > 1, \tau \leq T \tag{10}$$

It should also be noted that vehicle routing, which is fundamentally an NP-hard combinational optimization issue, is difficult in and of itself. More multiple binary variables are typically provided to create path-flow balance and start/end-at-locations requirements. Without the addition of new binary variables, the travel time is modelled in an innovative and compact manner. That is to say, only constraint (11) is required to ensure that the EV transportation between the TS roadways and the DN nodes meets the travelling time requirements. Due to the interaction between EV routing and other decisions and constraints, additional associated constraints, such as travel distance limitations, path-flow balance, and request satisfaction constraints, are fulfilled implicitly, or are reflected in the other constraints mentioned.

$$t^{arrival}_{i,g} + t^{travel}_{(i,j),g} - (1 - x^{Post}_{i,g,t})M \leq t^{arrival}_{j,g}, \forall i \in N^{CS}, \forall g \in G^{EV}_{ev}, \forall t \tag{11}$$

where $t^{arrival}_{i,g}$ and $t^{arrival}_{j,g}$ are the arrival time at node i and j, respectively. In order to ensure constraint (11) is feasible in the optimization, the Big-M approach is used; this is also known as the penalty technique. Mathematical formulation of this technique can be found in [25].

C. Dynamic Power Scheduling of EVs

Up to this stage, (post-event occurrence $t_e \sim t_{ir}$), it is assumed that all of the connected EVs are discharging their power to the grid via V2G mode, and that the number of disconnected EVs available that are willing to participate is determined in the preposition stage, and are optimally routed in the routing stage. Therefore, the decision made in the proceeding stages are integrated in this stage for optimal and dynamic power scheduling. The constraints involved in this stage are:

$$SOC_{g,t}^{EV} = SOC_{g,t-1}^{EV} + \left(\left[\eta^{CH} P_{g,\phi,t}^{CH}\right] - \left[\frac{P_{g,\phi,t}^{DISCH}}{\eta^{DISCH}}\right] - \left[x_{i,g,t}^{Post} CR\right] \right) \Delta t, \forall i \in N^{CS}, \forall g \in G_{ev}^{EV}, \phi \in \Phi, \forall t \tag{12}$$

$$SOC_{g,t}^{min} \leq SOC_{g,t}^{EV} \leq SOC_{g,t}^{max}, \forall g \in G_{ev}^{EV}, \forall t \tag{13}$$

$$0 \leq P_{g,\phi,t}^{DISCH} \leq P_{g,\phi,t}^{DISCH_{max}}, \forall g \in G_{ev}^{EV}, \phi \in \Phi, \forall t \tag{14}$$

$$0 \leq Q_{g,\phi,t}^{DISCH} \leq Q_{g,\phi,t}^{DISCH_{max}}, \forall g \in G_{ev}^{EV}, \phi \in \Phi, \forall t \tag{15}$$

$$0 \leq P_{g,\phi,t}^{CH} \leq P_{g,\phi,t}^{CH_{max}}, \forall g \in G_{ev}^{EV}, \phi \in \Phi, \forall t \tag{16}$$

$$x_{g,t}^{CH} + x_{g,t}^{DISCH} \leq \sum_{\forall i \in N^{CS}} x_{i,g,t}^{Post}, \forall g \in G_{ev}^{EV}, \forall t \tag{17}$$

$$SOC_{g,t}^{EV} = SOC_{g,t-1}^{EV} + \left(\left[\eta^{CH} P_{g,\phi,t}^{CH}\right] - \left[\frac{P_{g,\phi,t}^{DISCH}}{\eta^{DISCH}}\right] \right) \Delta t, \forall g \in G_{ev}^{EV}, \phi \in \Phi, \forall t \tag{18}$$

$$CR = D \times ECR \tag{19}$$

Constraint (12) limits the SOC of each EV g for each t. Constraint (13) ensures the g's SOC maximum and minimum limits. Constraints (14)-(16) limit the discharging active and reactive power, and charging active power, respectively. Constraint (17) guarantees that the charging and discharging actions or periods are always mutually exclusive states for each EV g, and that if it is not connected to the DN, it can neither charge nor discharge. Constraint (19) calculates the consumption rate CR of an EV's g travel for distance D in miles, multiplied by its characterized energy consumption rate ECR. It should be noted that the constraints associated with the EVs are applied to each EV g; for example, constraint (13) necessitates that each EV's SOC be maintained within its maximum ($SOC_{g,t}^{max}$) and minimum ($SOC_{g,t}^{min}$) rated values of its characterized SOC during the restoration process. As

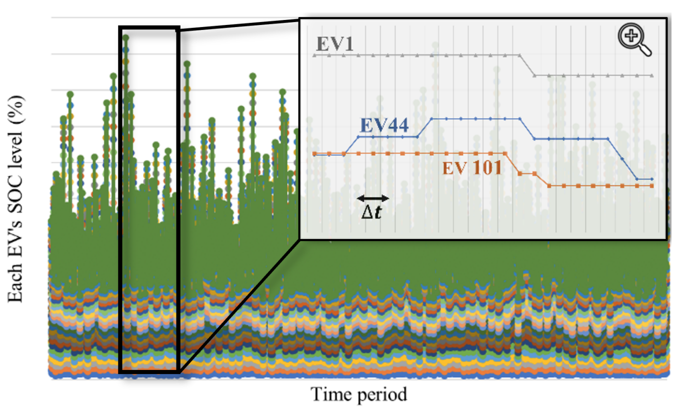

Fig. 2. Each EV's SOC at each time period during restoration.

shown in Fig. 2, each EV's SOC (for example, EV_1, EV_{44}, and EV_{101}) is maintained between the specified limits during the restoration period, as guaranteed by constraint (13). The other related constraints are held to the same concept. Alongside constraint (18), constraints (13)-(17) are also applied on the ESSs to ensure their functionality. Constraints (14) and (15) are applied to the DGs to limit their generated active and reactive power within the pre-specified limits. The following constraints are also involved in this stage: (1) unbalanced 3-phase optimal power flow constraints; (2) cold load pickup (CLPU) constraint; (3) transformer/voltage regulator and line kVA capacity constraints; (4) distributed energy resources (DERs), loads and lines connectivity constraints, as well as their associated operational constraints; (5) voltage limit constraints; (6) switching operation constraint; and (7) radiality constraint. Mathematical formulation of these constraints can be found in [27] and [28]. The objective function of this stage is formulated to minimize the load shedding cost and switching operation cost:

$$\min \sum_{\forall t} \left[\alpha \left(\sum_{\forall i} \sum_{\forall \phi} \left(1 - x_{l,t}^{L}\right) P_{i,\phi,t}^{L} \right) + \beta \left(\sum_{\forall (i,j)} x_{(i,j),t}^{SW} \right) \right], \forall t \in T, \forall i \in N, \forall \phi \in \Phi \tag{20}$$

where α and β are constants representing the load shedding cost and switching operation cost, respectively. $x_{(i,j),t}^{SW}$ is a binary variable indicating whether the switch in line (i,j) is operated ($x_{(i,j),t}^{SW} = 1$) at time t, otherwise it is ($x_{(i,j),t}^{SW} = 0$).

III. Case Studies

This section demonstrates the proposed EV proactive prepositioning, dynamic routing, and power scheduling framework on an IEEE 123-node test system with two case studies (i.e., Case I and Case II). In Case I, namely Proposed Strategy, the innovative framework described in Section II was applied. The EVs were prepositioned in a less coordinated manner in Case II, namely Benchmark. It was assumed for both cases that 90% of the EV users agreed to participate in the restoration processes. The problem was solved in 22.9 minutes for Case I and 31.2 minutes for Case II. The solution gap involved in solving this strategy was therefore set at 0.01%. As shown in Fig 3., the solution gap in solving Case I at the first iteration was more than that of the benchmark, due to the incorporation of the EVs' coordination, however the gap was reduced sooner, due to the coordination of the EVs. In both cases, it was assumed that the system had one EES with a 500kW/776kWh capacity, and one DG with a 800kW/600kVar capacity. It was also assumed that the system had 34 charging stations with different ratings and connection status, based on the assessment made by DNO and CSO. CSs have different capacities, namely their number of charging slots. Due to the lack of EV technical data available, the real data of each EV, including the SOC, charging, and discharging power ratings were collected from multiple confidential sources. The location of the charging stations and EVs were randomly determined

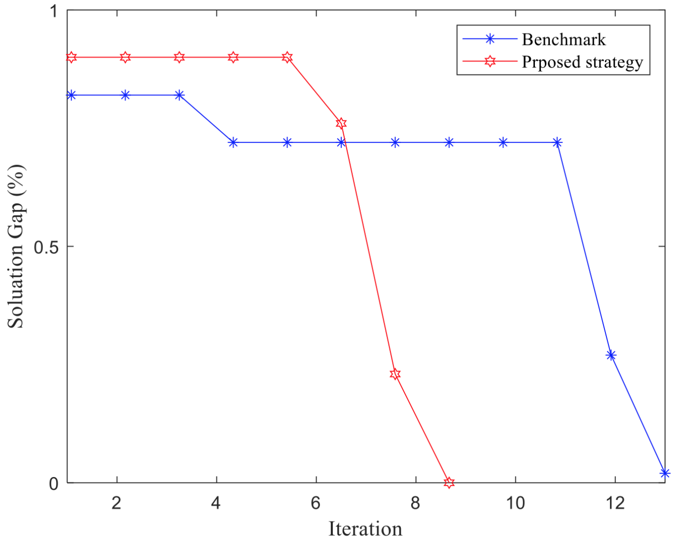

Fig. 3. Relative solution gap in each iteration.

using the MATH/Trig function, and could discharge energy to their local loads located at the same node if the line(s) connected to it was damaged. In both cases, a scenario was considered with 12 damaged lines that were assumed to be repaired in the order listed in Table II. As shown in Fig. 4., the

TABLE II
TIME SEQUENCE OF THE REPAIRS FOR DAMAGED LINES

Time	**1**	**2**	**3**	**4**	**5**	**6**
Line	1-7	15-16	19-20	57-58	58-58	98-99
Time	**8**	**10**	**13**	**14**	**16**	**19**
Line	82-83	44-45	68-71	67-68	36-39	23-25

well-coordinated EVs achieved better system restoration, due to the innovative three-stage optimization. It demonstrated that the sum of the weighted surviving load was higher in the early post-event stage. Furthermore, as a result of the innovative routing described in this paper, the amount of restored load in Case I in the middle stage (namely, from $t = 9$ to $t = 18$) was greatly enhanced. Also, the amount of demand grew significantly after , because the DN's lines were fully repaired, specifically when lines 23-25 were assumed to be repaired. It should be noted that the substation was assumed to be out of service for the entire duration of the restoration; this assumption confirmed the strategy's robustness further. Also, the proactive prepositioning stage presented in this article was demonstrably more resilient, since the overall sum of load surviving at $t = 1, 2, 3$ was higher than that of the benchmark. The system was assumed to have six new remote-controlled switches (RCSs). As shown in Table III, utilizing well-coordinated EVs could restore loads 8.7% higher than using EVs in a less coordinated manner, saving around 20% of the restoration cost. Fig. 5 shows the SOC of the ESS and the EVs, the DG active power output, and the total DN's load at each t, which is included in Fig. 5 for reference. The total

TABLE III
OBJECTIVE VALUE OF EACH CASE STUDY

Case	**Restored load**	**Restoration cost**	**RCS actions**
I	48741.9 kW	\$129,517.5	6
II	44861.8 kW	\$155,290.9	7

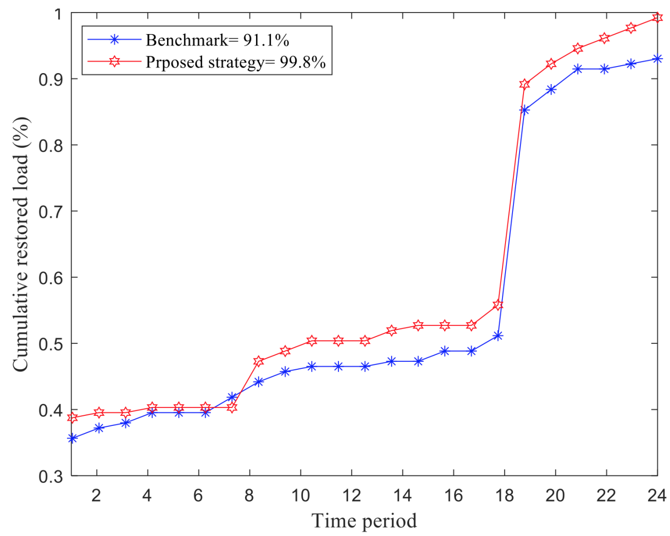

Fig. 4. Total sum of restored load (%) at each time period (t).

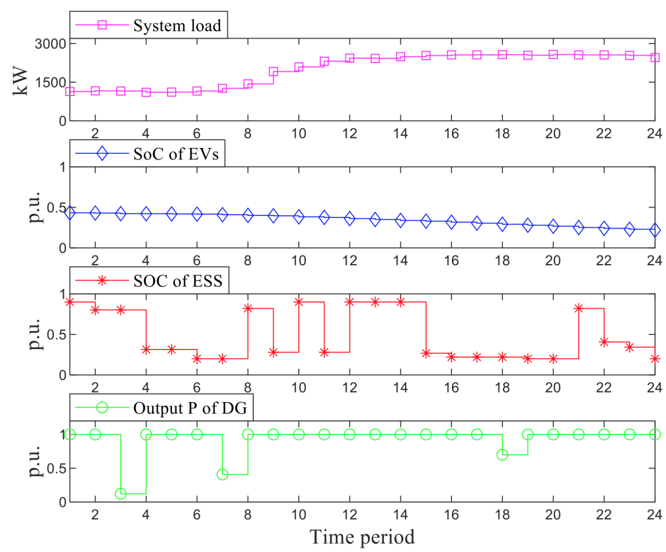

Fig. 5. System load, total SOC of the EVs, SOC of the ESS, and active power output of the DG in each time period.

SOC of the EVs for the restoration period was flat, due to the way of coordinating their charging and discharging timings. The ESS could compensate for the active power generated and the demand mismatch; in the meantime, the DG could be utilized to keep the total SOC decreasing in a flat pattern to maintain the restored load and prevent it from being shed after restoration, in case of a prolonged power outages. The coordination proposed amongst the EVs could also lower the

RCSs' actions, where the proposed strategy's RCS actions were less than those in the benchmark, as shown in Table IV.

TABLE IV
DYNAMIC NETWORK RECONFIGURATION OF THE DN

Time	RCS actions (Case I)	RCS actions (Case II)
3	Close line 1-7	
5	Open line 13-152	
7	Close line 18-138	Close line 150-149
8	Open line 87-89	Close line 18-138
9	Close line 13-152	
18	Close line 87-89	Open line 23-25
19	− − − − − − − −	Close line 23-25

IV. Conclusion

This study presented a three-stage optimization framework for implementing the robust prepositioning, dynamic routing, and scheduling of EVs in a smart DN and TS, with the aim of reducing the cost of restoration. For the first time, it proposed a novel travelling model of EVs, which significantly reduced computing time demand while maintaining the accuracy. Each EV user's decision to participate in the process was integrated implicitly into the proposed framework to improve the effectiveness. Findings of the investigations suggest that using well-coordinated EVs potentially restore loads than using EVs in a less coordinated manner, with a significant cost savings. The real information interchange between the DNO and the CSOs indicated that the sum of the weighted surviving load can be improved, due to the unique coordination between the three stages of the proposed approach.

Acknowledgment

This work was financially supported in part by Taibah University through its sponsorship of the author A. Alghamdi.

References

[1] President's Council of Economic Advisers U.S. Dept. Energy's Office of Electricity Energy Reliability, "Economic benefits of increasing electric grid resilience to weather outages," U.S. Dept. Energy, Executive Office President, Washington, DC, USA, Rep., 2013.

[2] R. J. Campbell, "Weather-related power outages and electric system resiliency," Congressional Res. Service, Washington, DC, USA, Rep. R42696, 2012.

[3] Improving Electric Grid Reliability and Resilience: Lessons Learned From Superstorm Sandy and Other Extreme Events, GridWise Alliance, Washington, DC, USA, 2013.

[4] 'IEEE Standard for Interconnection and Interoperability of Distributed Energy Resources with Associated Electric Power Systems Interfaces–Amendment 1: To Provide More Flexibility for Adoption of Abnormal Operating Performance Category III', IEEE Std 1547a-2020 (Amendment to IEEE Std 1547-2018), pp. 1–16, Apr. 2020, doi: 10.1109/IEEESTD.2020.9069495.

[5] R. Billinton and R. N. Allan, Reliability Evaluation of Power Systems, 2nd ed. New York, NY, USA: Plenum, 1996.

[6] "Enhancing grid resilience with integrated storage from electric vehicles," EAC U.S. Dept. Energy, Washington, DC, USA, Rep., 2018.

[7] N. Gordon-Bloomfield. (Mar. 2014). Nissan, Mitsubishi, Toyota Turn Electric Cars into Backup Batteries. [Online]. Available: http://www.greencarreports.com/news/1063565nissan-......-batteries.

[8] B. Ozpineci, "Technology development: Updates, challenges and opportunities," presented at the EAC SGS, May 2018.

[9] A. Briones et al., Vehicle-to-Grid (V2G) Power Flow Regulations and Building Codes Review by the AVTA, Idaho Nat. Lab., Idaho Falls, ID, USA, Sep. 2012.

[10] G. Putrus, et al., "Interreg North Sea Region SEEV4-city project: Summary of the state-of-the-art report," SEEV4-City Consortium, Rep., 2018.

[11] "Enhancing distribution resiliency: Opportunities for applying innovative technologies," Elect. Power Res. Inst., Palo Alto, CA, USA, Rep. 1026889, Jan. 2013

[12] National Academies of Sciences, Engineering, and Medicine, Enhancing the Resilience of the Nation's Electricity System. Washington, DC, USA: Nat. Acad. Press, 2018.

[13] "The resilience of the electricity system," Sci. Technol. Select Committee, House of Lords, London, U.K., Rep., 2015.

[14] N. A. of S. Medicine Engineering, and, D. on E. and P. Sciences, B. on E. and E. Systems, and C. on E. the R. of the N. E. P. T. and D. System, Enhancing the Resilience of the Nation's Electricity System. National Academies Press, 2017.

[15] Z. Yang, P. Dehghanian, and M. Nazemi, "Enhancing Seismic Resilience of Electric Power Distribution Systems with Mobile Power Sources," in 2019 IEEE Industry Applications Society Annual Meeting, Sep. 2019, pp. 1–7. doi: 10.1109/IAS.2019.8912010.

[16] S. Lei, C. Chen, H. Zhou, and Y. Hou, "Routing and Scheduling of Mobile Power Sources for Distribution System Resilience Enhancement," IEEE Trans. Smart Grid, vol. 10, no. 5, pp. 5650–5662, Sep. 2019, doi: 10.1109/TSG.2018.2889347.

[17] B. Li, Y. Chen, W. Wei, S. Huang, and S. Mei, "Resilient Restoration of Distribution Systems in Coordination With Electric Bus Scheduling," IEEE Trans. Smart Grid, vol. 12, no. 4, pp. 3314–3325, Jul. 2021, doi: 10.1109/TSG.2021.3060801.

[18] M. Al-Muhaini, "Electric Vehicle Markov-Based Adequacy Modeling for Electric Microgrids," IEEE Access, vol. 8, pp. 132721–132735, 2020, doi: 10.1109/ACCESS.2020.3010614.

[19] Z. Guo, S. Lei, Y. Wang, Z. Zhou, and Y. Zhou, "Dynamic distribution network reconfiguration considering travel behaviors and battery degradation of electric vehicles," in 2017 IEEE Power Energy Society General Meeting, Jul. 2017, pp. 1–5. doi: 10.1109/PESGM.2017.8274475.

[20] S. Mohsen, M. H. Nezhad, A. Fereidunian, H. Lesani, and M. H. Gavgani, "Enhancement of self-healing property of smart grid in islanding mode using electric vehicles and direct load control," in 2014 Smart Grid Conference (SGC), Dec. 2014, pp. 1–6. doi: 10.1109/SGC.2014.7090860.

[21] B. Chen, J. Wang, X. Lu, C. Chen, and S. Zhao, "Networked Microgrids for Grid Resilience, Robustness, and Efficiency: A Review," IEEE Trans. Smart Grid, vol. 12, no. 1, pp. 18–32, Jan. 2021, doi: 10.1109/TSG.2020.3010570.

[22] D. K. Mishra, M. J. Ghadi, A. Azizivahed, L. Li, and J. Zhang, "A review on resilience studies in active distribution systems," Renew. Sustain. Energy Rev., vol. 135, p. 110201, Jan. 2021, doi: 10.1016/j.rser.2020.110201.

[23] Y.-W. Chung, B. Khaki, T. Li, C. Chu, and R. Gadh, "Ensemble machine learning-based algorithm for electric vehicle user behavior prediction," Appl. Energy, vol. 254, p. 113732, Nov. 2019, doi: 10.1016/j.apenergy.2019.113732.

[24] A. Hussain and P. Musilek, "Resilience Enhancement Strategies For and Through Electric Vehicles," Sustain. Cities Soc., vol. 80, p. 103788, May 2022, doi: 10.1016/j.scs.2022.103788.

[25] E. Hadian, H. Akbari, M. Farzinfar, and S. A. Saeed, "Optimal Charging/Discharging Control of Electric Vehicle Charging Station Considering Grid Resiliency," International Journal of Industrial Electronics, Control and Optimization, vol. 4, p. 12, 2021, doi: 10.22111/IECO.2021.37211.1335.

[26] Bedekar, P.P., Bhide, S.R. and Kale, V.S., 2009. Optimum time coordination of overcurrent relays in distribution system using Big-M (penalty) method. WSEAS Transactions on Power Systems, 4(11), pp.341-350.

[27] A. Arif, Z. Wang, C. Chen, and J. Wang, "Repair and Resource Scheduling in Unbalanced Distribution Systems Using Neighborhood Search," IEEE Trans. Smart Grid, vol. 11, no. 1, pp. 673–685, Jan. 2020, doi: 10.1109/TSG.2019.2927739.

[28] B. Chen, Z. Ye, C. Chen, and J. Wang, "Toward a MILP Modeling Framework for Distribution System Restoration," IEEE Trans. Power Syst., vol. 34, no. 3, pp. 1749–1760, May 2019, doi: 10.1109/TPWRS.2018.28853.